J. Membrane Biol. 105, 33–43 (1988)

The Journal of
Membrane Biology

Osmotic Gradient Dependence of Osmotic Water Permeability in Rabbit Proximal Convoluted Tubule

Christine A. Berry and A.S. Verkman
Departments of Physiology and Medicine, and Cardiovascular Research Institute, University of California, San Francisco, California 94143

Summary. To assess steady-state transepithelial osmotic water permeability (P_f), rabbit proximal convoluted tubules were perfused in vitro with the impermeant salt, sodium isethionate at 26°C. Osmotic gradients ($\Delta\Pi$) were established by varying the bath concentration of the impermeant solute, raffinose. When lumen osmolality was 300 mOsm and bath osmolality was 320, 360 and 400 mOsm, apparent P_f decreased from 0.5 to 0.10 to 0.08 cm/sec, respectively. Similar data were obtained when lumen osmolality was 400 mOsm. Five possible causes of the $\Delta\Pi$ dependence of apparent P_f were considered experimentally and/or theoretically: (1) external unstirred layer (USL); (2) cytoplasmic USL; (3) change in surface area; (4) saturation of water transport; (5) down-regulation of P_f. Apparent P_f was inhibited 83% by *p*-chloromercuribenzene sulfonate (*p*CMBS) at 20 mOsm, but not at 60 mOsm $\Delta\Pi$, suggesting presence of a serial barrier resistance to water transport. Increases in perfusate or bath solution flow rate and viscosity did not alter apparent P_f, ruling out an external USL. A simple cytoplasmic USL, described by a constant USL thickness and solute diffusion coefficient, could not account for the $\Delta\Pi$ dependence of apparent P_f according to a mathematical model. The activation energy (E_a) for apparent P_f increased from 7.0 to 12.5 kcal/mol when $\Delta\Pi$ was increased from 20 to 60 mOsm, not consistent with a simple USL or a change in membrane surface area with transepithelial water flow. These findings are most consistent with a complex cytoplasmic USL, where the average solute diffusion coefficient and/or the area available for osmosis decrease with increasing $\Delta\Pi$. These results (1) indicate that true P_f (at physiologically low $\Delta\Pi$) is very high (>0.5 cm/sec) in the rabbit proximal tubule; (2) provide an explanation for the wide variation in P_f values reported in the literature using different $\Delta\Pi$, and (3) suggest the presence of a flow-dependent cytoplasmic barrier to water flow.

Key Words osmotic water permeability · osmotic gradient dependence · external unstirred layer · cytoplasmic unstirred layer · mathematical model · kidney proximal tubule

Introduction

An explicit value for the transepithelial osmotic water permeability (P_f) of the proximal convoluted tubule (PCT) is required for quantitative treatment of proximal volume reabsorption. In the last two decades P_f in the rabbit PCT has been reported to be in the range between 0.04 to 0.7 cm/sec (Berry, 1983). Unstirred layers (USL) have been suggested to explain this wide range of P_f (Berry, 1983).

The purpose of the present studies was to estimate the true P_f of the PCT, taking into account extra- and intraepithelial USL. We find that the apparent P_f varies inversely with the osmotic gradient ($\Delta\Pi$). Possible causes of the $\Delta\Pi$ dependence of apparent P_f were examined by a series of experimental protocols. The data are not consistent with (1) an external USL, (2) a simple cytoplasmic USL, (3) a change in the surface area, and (4) a saturable, symmetrical water transport mechanism in parallel with a nonsaturable water transport mechanism. Theoretical and experimental analyses of the data are consistent with (1) a complex cytoplasmic USL in which the solute diffusion coefficient and/or the area available for flow decreases with increasing $\Delta\Pi$, and (2) physiological down-regulation of P_f. We conclude that in the rabbit PCT the $\Delta\Pi$ dependence of apparent P_f accounts for the wide variation of reported P_f, and that the true P_f, if extrapolated to zero $\Delta\Pi$, is greater than 0.5 cm/sec.

Materials and Methods

Isolated segments of rabbit PCT were dissected and perfused as described previously (Berry, 1983, 1985). Briefly, kidneys from female New Zealand white rabbits were cut in coronal slices. Individual PCT were dissected in cooled (4°C) perfusion solution containing (mM) 150 sodium isethionate, 5 potassium isethionate, 4 dibasic sodium phosphate, 2 calcium gluconate, 1 magnesium sulfate, 1 butyric acid. Butyric acid was used as the metabolic substrate; Harris et al. (1982) showed that butyric acid supplementation provides adequate ATP during periods of high metabolic demand. The perfusion solution was equilibrated with 100% O_2, adjusted to pH 7.4 and was approximately 300 mosmol/kg H_2O (mOsm).

Tubules were transferred to a specially constructed bath of approximately 1.2 ml with a temperature range of 10–50°C (Berry, 1985). Bath temperature was maintained at 26°C unless otherwise specified. The bath solution was continuously changed by flowing bath fluid through the chamber at 1 ml/min unless otherwise stated. This arrangement provided good mixing of the bath solution (Berry, 1985). Bath mixing was examined visually using 0.8 μ polystyrene beads (Sigma Chemical Co., St. Louis, MO). At 250× magnification and 0.4 ml/min bath flow rate, beads were uniformly distributed in the bathing solution and in the region directly adjacent to the basement membrane of the PCT. Therefore, bath mixing appeared complete and no excluded volume or macroscopic external USL could be detected.

Perfusion Solutions

Dissected tubules between 0.7 and 1.6 mm in length (average 1.04 ± 0.04 mm, SEM, n = 27) were perfused at rates 25–70 nl/min (average 41 ± 3 nl/min, n = 27) with perfusion solution containing ^{14}C-inulin (New England Nuclear, 100 μCi/ml perfusate). In the absence of an osmotic gradient, tubules were bathed in perfusion solution (*see above*) containing 6 g/dl bovine serum albumin and 4 mM calcium gluconate. To equalize the osmolalities of the bathing solution and the perfusate, water was added to the bathing solution. With these osmotically adjusted solutions, the ratio of collected fluid to perfused fluid inulin radioactivity was 0.999 ± 0.008 (n = 8, 26°C).

For determination of apparent P_f, a transepithelial osmotic gradient was produced by addition of varying amounts of raffinose to the bath solution. For examination of the gradient dependence, 20, 60 and 100 mOsm gradients were tested. For examination of the effect of *p*-chloromercuribenzene sulfonate (*p*CMBS), only 20 and 60 mOsm gradients were tested. For examination of the effect of luminal perfusion rate and bath exchange rate and of bath viscosity, only a 60-mOsm gradient was tested.

For examination of the symmetry of the osmotic gradient dependence, $\Delta\Pi$ was generated by addition or subtraction of 20 and 60 mOsm sodium isethionate. This was necessary because raffinose was not present in the control perfusion solution and, therefore, could not be subtracted. Because of uncertainties regarding the reflection coefficient of this salt, these data are not directly comparable to all other data obtained using raffinose as the osmotic agent.

Protocol

The tubules were allowed to equilibrate for 15 min in the absence of an osmotic gradient before collections were begun. Collections, usually four, were made every 1–3 min with a 75-nl constant volume pipette. At the beginning and the end of each protocol, collections were made in the absence of an osmotic gradient. Only those tubules in which the collected/perfused inulin concentration ratio was between 0.99 and 1.01 were included in the data analysis. This strict procedure was necessary because the maximum collected/perfused inulin concentration ratio for 20-mOsm gradients (at osmotic equilibrium) was ~1.07 (320/300). In general, osmotic equilibration was <50% and the collected/perfused inulin ratio for the 20-mOsm gradient was ~1.03.

Analysis

Collections were put into a vial containing a 1:4 mixture of acetic acid/Aquasol (New England Nuclear) for liquid scintillation counting (Tri-Carb 460C, Packard, Downers Grove, IL). A mean value for P_f was determined from the three to four collections during a given period in a given tubule.

Calculations

In the presence of impermeant solutes collected fluid osmolality was calculated from the product of the collected/perfused inulin concentration ratio and the perfusate osmolality. The assumption of solute impermeability was validated by comparing the collected fluid osmolality calculated using the collected inulin concentration ratio with that measured using the method described by Ramsay and Brown (1955). The two methods agreed to within one mOsm. The ratio of the inulin method/Ramsay-Brown method was 0.998 ± 0.004 (n = 3). Apparent P_f values were calculated using the equations developed by DuBois, Verniory and Abramow (1976) and Al-Zahid et al. (1977).

Statistics

Data are expressed as mean ± SE. The statistical significance for mean paired differences was assessed using the Student t-test.

Results

Dependence of Apparent P_f on the Osmotic Gradient

Nonequilibrium thermodynamics predicts a linear relationship between transepithelial volume flux (J_v) and osmotic gradient. The proportionality coefficient is $P_f(V_w/RT)$, where V_w is the partial molar volume of water, R the gas constant, and T absolute temperature. Because of partial dissipation of the osmotic gradient along the length of the tubule, the log mean osmotic gradient ($\overline{\Delta\Pi}$) was taken as a measure of the osmotic gradient. When 5 PCT were perfused with varying concentrations of sodium isethionate, Fig. 1 shows that the relationship between the J_v and $\overline{\Delta\Pi}$ was symmetrical, but nonlinear. J_v obtained at the higher $\overline{\Delta\Pi}$ is lower than predicted for a constant P_f. In Fig. 1 perfusate osmolality was constant at ~300 mOsm. Apparent P_f decreased from 0.13 ± 0.03 to 0.06 ± 0.01 cm/sec when the bathing solution was 20 and 60 mOsm *hypo*tonic to the perfusate (mean paired difference: 0.08 ± 0.03, $P < 0.05$). When the bathing solution was varied from 20 to 60 mOsm *hyper*tonic to the perfusate, apparent P_f decreased similarly from 0.15 ± 0.04 to 0.03 ± 0.01 cm/sec (mean paired difference: 0.011 ± 0.04, $P < 0.05$). There was no signifi-

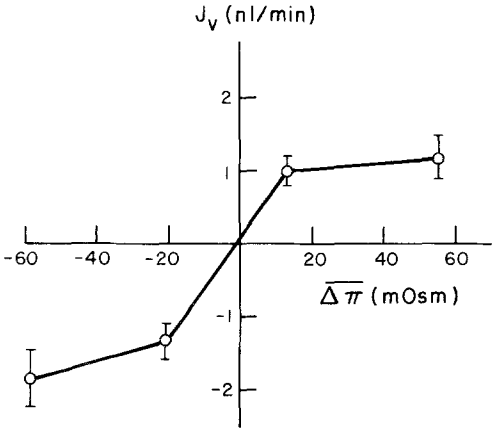

Fig. 1. Dependence of volume absorption (J_v, nl/mm min) on the log mean osmotic gradient ($\overline{\Delta\Pi}$, mOsm). Each point represents mean ± SEM of 5 PCT. $\Delta\Pi$ was varied by altering the concentration of sodium isethionate

cant difference between apparent P_f's at identical but oppositely directed $\overline{\Delta\Pi}$ (mean paired difference: $\overline{\Delta\Pi}$ [20 mOsm] 0.02 ± 0.06, $P > 0.05$; $\overline{\Delta\Pi}$ [60 mOsm] 0.02 ± 0.01, $P > 0.05$).

The $\overline{\Delta\Pi}$ dependence of apparent P_f was examined over a wider range of $\overline{\Delta\Pi}$ by adding varying concentrations of raffinose to the bathing solution. Table 1 shows the dependence of apparent P_f on the initial osmotic gradient ($\Delta\Pi_o$) for perfusate osmolarities of 300 and 400 mOsm. For the 300 mOsm perfusate (Table 1, left) apparent P_f was 0.50 ± 0.12, 0.10 ± 0.02, and 0.08 ± 0.03 cm/sec. The apparent P_f at a $\Delta\Pi_o$ of 20 mOsm was significantly higher than that at $\Delta\Pi_o$ of 60 and 100 mOsm.[1]

To determine whether the apparent $\Delta\Pi$ dependence of measured P_f was due to changes in $\Delta\Pi$ rather than to changes in absolute osmolarity which might decrease cell volume or alter the membrane directly, P_f was measured using a 400 mOsm perfusate and 400 mOsm + $\Delta\Pi_o$ bath. In 4 PCT perfused with 400 mOsm sodium isethionate and 20, 60 and 100 mOsm raffinose gradients, apparent P_f was 0.37 ± 0.14, 0.05 ± 0.02, and 0.4 ± 0.01 cm/sec. These data show a $\Delta\Pi$ dependence of apparent P_f similar to that obtained using a 300 mOsm sodium isethionate perfusate, suggesting that the $\Delta\Pi$ dependence of apparent P_f is related to $\Delta\Pi$. The small, but not

[1] The variation in apparent P_f is similar to that obtained using sodium isethionate gradients. The ratio of apparent P_f at 20 mOsm to apparent P_f at 60 mOsm was 4.4 using sodium isethionate and 5.0 using raffinose. However, the absolute value of apparent P_f is smaller for sodium isethionate. There is no obvious reason for this discrepancy, but it may be due to differing reflection coefficients for sodium isethionate and raffinose.

Table 1. Dependence of apparent P_f on initial osmotic gradient ($\Delta\Pi_o$)

Perfusate osmolality (mOsm)	Apparent P_f (cm/sec)	
	300	400
$\Delta\Pi_o$ (mOsm)		
20	0.50 ± 0.12	0.37 ± 0.14
60	0.10 ± 0.02[a]	0.05 ± 0.02[b]
100	0.08 ± 0.03	0.04 ± 0.01

[a] Significantly different from $\Delta\Pi_o$ (20 mOsm, perfusate osmolality 300 mOsm); mean paired difference: 0.40 ± 0.11, $P < 0.001$, $n = 6$.

[b] Significantly different from $\Delta\Pi_o$ (20 mOsm, perfusate osmolality 400 mOsm); mean paired difference: 0.32 ± 0.13, $P < 0.05$, $n = 4$.

Table 2. Effect of *p*CMBS on apparent P_f

$\Delta\Pi_o$ (mOsm)	Apparent P_f (cm/sec)	
	20	60
−*p*CMBS	0.29 ± 0.09	0.05 ± 0.01
+*p*CMBS	0.04 ± 0.02[a]	0.06 ± 0.01[b]
% Inhibition	83 ± 32	0 ± 40

[a] Mean paired difference: 0.25 ± 0.09, $P < 0.05$, $n = 6$.

[b] Mean paired difference: 0.01 ± 0.02, $P > 0.05$, $n = 6$.

significant decreases in P_f with the 400 mOsm perfusate may be related to a small decrease in cell volume resulting in an increase in cytoplasmic viscosity (*see* Discussion).

Effect of 2 mM *p*CMBS on the $\Delta\Pi$ Dependence of Apparent P_f

A possible explanation for the $\Delta\Pi$ dependence of apparent P_f is the presence of a USL. To test the hypothesis that apparent P_f is membrane-limited at small $\Delta\Pi$ and nonmembrane-limited at larger $\Delta\Pi$, the effect of 2 mM lumen and bath *p*CMBS on apparent P_f was examined at 20 and 60 mOsm raffinose gradients (Table 2). In 6 PCT apparent P_f determined using a 20 mOsm raffinose gradient was 0.29 ± 0.09 in the absence of *p*CMBS and 0.04 ± 0.02 cm/sec in the presence of *p*CMBS representing 83% inhibition. In contrast, when apparent P_f was determined using a 60 mOsm raffinose gradient, apparent P_f was not significantly influenced by the addition of *p*CMBS. These data are consistent with the view that transcellular osmosis involves two resistances in series: membrane and USL. At a $\Delta\Pi_o$ of

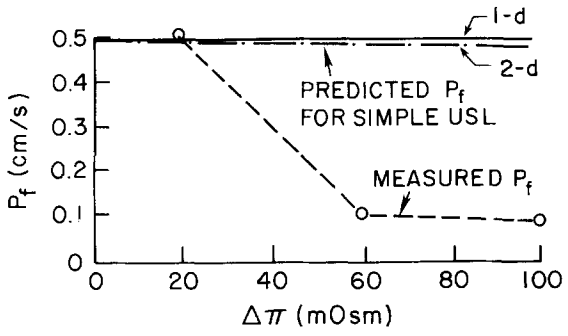

Fig. 2. Calculated dependence of apparent P_f on $\Delta\Pi$ in the presence of a simple cytoplasmic unstirred layer. Curves were calculated from Eqs. (A3) and (A4) (one-dimensional USL) and (A8) and (A4) (two-dimensional USL) with $C_1 = 300$ mOsm, $C_2 = 300 + \Delta\Pi$ mOsm, $S = 6.3 \times 10^{-4}$ cm²/mm, $V_w = 18$ cm³/mole, $P_f^m = 0.5$ cm/sec (or equivalently, true transepithelial P_f of 1 cm/sec), $D = 5 \times 10^{-6}$ cm²/sec, $d = 5\,\mu$, $r_1 = 10\,\mu$ and $r_2 = 20\,\mu$. Measured apparent P_f data are shown for comparison

20 mOsm, osmosis is predominately restricted by a *p*CMBS-sensitive, membrane pathway. At a $\Delta\Pi_o$ of 60 mOsm, osmosis is predominately *p*CMBS-insensitive and nonmembrane limited.

Evaluation of External Unstirred Layers

The presence of an external USL in series with one or both of the cell membranes (between the luminal solution and the apical membrane and/or the bath solution and the basolateral membrane) would predict that apparent P_f might be sensitive to perfusate flow rate and bath solution mixing rate and viscosity. Increased mixing rate should increase apparent P_f by decreasing USL thickness. Increasing solution viscosity should decrease apparent P_f by decreasing solute diffusion coefficients in the USL. These effects would be more apparent at larger $\Delta\Pi$; therefore, a 60 mOsm raffinose gradient was used.

Effect of Bath Flow Rate on Apparent P_f

Increasing bath flow rate 25-fold, from 0.4 to 10 ml/min, did not significantly increase apparent P_f. Apparent P_f was 0.07 ± 0.03 (0.4 ml/min) and 0.07 ± 0.05 cm/sec (10 ml/min) (mean paired difference: 0.01 ± 0.02, $P > 0.05$, $n = 4$).

Effect of Luminal Flow Rate on Apparent P_f

Changing luminal perfusion rate from 40 to 12 and back to 40 nl/min did not significantly alter apparent P_f. Apparent P_f was 0.03 ± 0.01, 0.04 ± 0.01, and 0.04 ± 0.01 cm/sec (mean paired differences: 0.01 ± 0.01, $P > 0.05$, $n = 6$).

Effect of Increasing Bath Viscosity on Apparent P_f

Bath viscosity was increased by addition of high molecular weight dextran (77,500 daltons) and was measured using an Oswald viscometer. Increasing bathing solution viscosity >10-fold, from 0.010 to 0.108 Poise with 2 mM dextran did not significantly decrease apparent P_f. Apparent P_f was 0.05 ± 0.02 and 0.04 ± 0.02 cm/sec (mean paired difference: 0.01 ± 0.01, $P > 0.05$, $n = 4$).[2]

Evaluation of Cytoplasmic Unstirred Layers

The effect of a 'simple' cytoplasmic USL on the $\Delta\Pi$ dependence of apparent P_f was calculated (*see* Appendix). For a simple USL, solute diffusion and the area available for volume flow are assumed to be independent of transepithelial volume flow. The calculation is based on the steady-state solution to the convection-diffusion equation applied with boundary conditions appropriate for a cell. Equations were solved both in one dimension and in two dimensions, to closely approximate tubule geometry.

As shown in Fig. 2, the hypothesis that a simple cytoplasmic USL can account for the measured dependence of P_f on $\Delta\Pi$ is wrong. For calculations performed in both one and two dimensions with parameters chosen from the PCT (*see* legend to Fig. 2), there is only a slight dependence of apparent P_f on $\Delta\Pi$, far less than that measured experimentally. Qualitatively, the reason for this finding is that there is a roughly proportionate effect of transepithelial volume movement on solute polarization within the USL for any value of transepithelial volume movement (*see* Discussion). This finding holds for a wide range of parameters tested in one and two dimensions, and for a simple external USL with or without a simple cytoplasmic USL.

[2] Although increasing solution viscosity with high molecular weight dextran is a standard method to increase solution viscosity with a minimal increase in solution osmolarity, it has been questioned that dextran addition does not change microscopic solute diffusion coefficients to the same degree that it increases bulk viscosity (S.D. Levine, *private communication;* Wang, 1954). If this is correct, the conclusion that the dextran data rule out external USL's is weakened.

Table 3. Effect of temperature on apparent P_f

$\Delta\Pi_o$ (mOsm)	Apparent P_f (cm/sec)	
	20	60
20°C	0.15 ± 0.02	0.04 ± 0.01
39°C	0.32 ± 0.03	0.16 ± 0.06
E_a (kcal/mole)	7.0 ± 0.4[a]	12.5 ± 2.0[a]

[a] Unpaired difference: 5.5 ± 2.0, $P < 0.025$, $n(20) = 5$ and $n(60) = 10$.

ΔΠ Dependence of Activation Energy for Apparent P_f

The activation energy (E_a) for apparent P_f at 20 and 60 mOsm gradients was measured to distinguish among causes for the ΔΠ dependence of P_f. If apparent P_f decreases with increasing ΔΠ because of a decrease in tubule surface area with increasing transepithelial volume flow, there should be no effect of ΔΠ on E_a because the intrinsic properties of the 'folded' and 'unfolded' membrane should be identical. If the ΔΠ dependence of apparent P_f is due to an increasing relative contribution of a *simple* cytoplasmic USL with increasing ΔΠ, then E_a is expected to approach the value obtained for solute diffusion in aqueous solution, 4.5–5 kcal/mole at large ΔΠ. E_a at small ΔΠ would depend on the mechanism of water transport: water movement through a lipid pathway is expected to have an E_a of 10–20 kcal/mole; water movement through a porous, water-filled channel is expected to have an E_a of <5 kcal/mole. However, if the ΔΠ dependence of apparent P_f is due to an increasing relative contribution of a *complex* cytoplasmic USL, then it is not a priori possible to predict the E_a at high ΔΠ.

The effect of temperature on apparent P_f is shown in Table 3. Apparent P_f was measured at 20 and 39°C at 20 and 60 mOsm gradients. Only two, widely displaced temperatures were used to obtain significant differences in apparent P_f at a ΔΠ of 20 mOsm (*see* Materials and Methods). Apparent E_a increased significantly from 7.0 ± 0.4 kcal/mole when ΔΠ was 20 mOsm to 12.5 ± 2.0 kcal/mole when ΔΠ was 60 mOsm ($P < 0.025$).

Discussion

The purpose of the present studies was to measure the true transepithelial P_f in the rabbit PCT. Apparent P_f was found to vary inversely with ΔΠ. ΔΠ dependence has been observed in a variety of epithelia and has most frequently been attributed to a

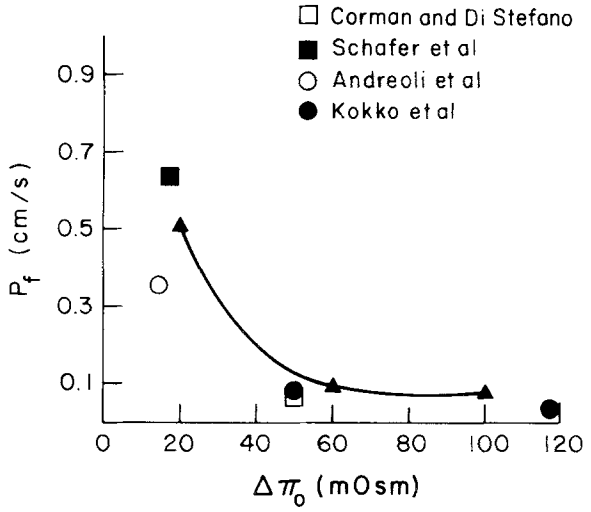

Fig. 3. Comparison of present data (solid triangles, solid line) with previously obtained values of transepithelial osmotic water permeability (P_f, cm/sec) as a function of initial osmotic gradient ($\Delta\Pi_o$, mOsm)

USL providing a resistance to water flow in series with the plasma membranes. Five mechanisms for the ΔΠ dependence were considered experimentally and/or theoretically: (1) external USL; (2) cytoplasmic USL; (3) flow-dependent change in surface area; (4) saturation of a water transport pathway; and (5) physiologic down-regulation of a water transport pathway. Nonlinear osmosis and its possible explanations will be considered in the following discussion.

ΔΠ Dependence of P_f in Rabbit Proximal Tubule

In the last two decades a wide range of values have been reported for transepithelial osmotic water permeability in the rabbit proximal tubule: 0.04 to 0.7 cm/sec. Three technical considerations have been suggested to account for the variation in reported P_f (Berry, 1983): (1) methods of measurement; (2) varying reflection coefficients for the osmotic probe; and (3) USL. In the present study apparent P_f was measured at initial osmotic gradients of 20, 60 and 100 mOsm raffinose eliminating causes (1) and (2) as explanations for variation in P_f. Nonetheless, a significant ΔΠ-dependence of apparent P_f was obtained (Table 1). Figure 3 shows a comparison of the present values for P_f as a function of $\Delta\Pi_o$ (filled triangles, solid line) with previous data. The ΔΠ dependence of P_f is a consistent observation. Those investigators who used small ΔΠ obtained high P_f (Andreoli, Schafer & Troutman, 1978; Schafer, Patlak & Andreoli, 1978) and those who used

large $\Delta\Pi$ obtained low P_f (Kokko, Burg & Orloff, 1971; Corman & DiStefano, 1983).

$\Delta\Pi$ Dependence of P_f (Nonlinear Osmosis)

Nonlinear osmosis has been described in a variety of epithelia: toad urinary bladder (Bentley, 1961); turtle bladder (Brodsky & Schilb, 1965); frog skin (House, 1974; Franz & Van Bruggen, 1967); fowl cloaca (Skadhauge, 1967); *Necturus* gallbladder (Persson & Spring, 1982); rabbit gallbladder (Diamond, 1966; Wright, Smulders & Tormey, 1972); dog gastric mucosa (Altamirano & Martinoya, 1966); frog intestine (Loeschke, Bentzel & Caaky, 1970); *Necturus* proximal tubule (Bentzel, Parsa & Hare, 1969); rat proximal tubule (Frömter et al., 1969; Ullrich et al., 1972); and rabbit proximal tubule (Capri-Medina, Gonzalez & Whittembury, 1983). In the early studies nonlinear osmosis was usually explained by such theories as flow-induced membrane deformation (Brodsky & Schilb, 1965), asymmetrical series-membrane effects (Kedem & Katchalsky, 1963; Ogilvie, McIntosh & Curran, 1963; Patlak, Goldstein & Hoffman, 1963), external USL (Dainty, 1963; Brodsky & Schilb, 1965), cytoplasmic USL (Dick, 1959) and osmotic and nonosmotic effects of the osmotic solutes (Earley, Sidel & Orloff, 1962; Dainty & Ginzburg, 1964). Illsley and Verkman (1986) added the possibility that saturation of the water transport mechanism might lead to nonlinear osmosis. However, most recent authors have used the arguments advanced by Diamond (1979; Barry & Diamond, 1984) and have invoked either external or cytoplasmic USL to explain the phenomena (Wright et al., 1972; Persson & Spring, 1982; Capri-Medina et al., 1983; Corman, 1985).

Role of USL in $\Delta\Pi$ Dependence of Apparent P_f

P_f can be underestimated in the presence of a USL. When the transepithelial water transport pathway consists of cell membranes in series with a USL, apparent P_f would be limited by two barriers to osmosis. Inhibition of osmotic water movement by *p*CMBS was observed only at low $\Delta\Pi_o$ (Table 2), where the cell membranes constitute the rate-limiting barriers to water permeation. At high $\Delta\Pi_o$ the inhibitory potency of *p*CMBS decreased (Table 2). Such a decreased sensitivity to *p*CMBS might occur because the rate-limiting barrier at high $\Delta\Pi_o$, the USL, is not *p*CMBS sensitive.

In addition to suggesting a USL, the large effect of *p*CMBS at 20 mOsm $\Delta\Pi$ gives some insight into the membrane water transport mechanism. In the red blood cell *p*CMBS inhibits water entrance through aqueous channels, presumably by binding to the sulfhydryl groups of the proteins that constitute the channel walls and thereby closing the channel (Macey, Daran & Farmer, 1972). Osmotic water permeability of the red cell is inhibited by about 90% by *p*CMBS (Macey et al., 1972). In the proximal tubule *p*CMBS has been shown to inhibit osmotic water permeability in luminal (Pratz, Ripoche & Corman, 1986; van Heeswijk and van Os, 1986) and basolateral (Whittembury et al., 1984; Meyer & Verkman, 1987) membranes and in rabbit proximal tubule cells (Meyer & Verkman, 1987) and to inhibit transepithelial (Berry, 1985) and basolateral membrane diffusional water permeability (Verkman & Wong, 1987) in rabbit PCT. *p*CMBS sensitivity has been taken as evidence for the existence of protein-bound aqueous channels in the cell membranes. If *p*CMBS does not inhibit paracellular osmotic water permeability, the high degree of *p*CMBS inhibition at low $\Delta\Pi_o$ provides strong evidence for a predominately (at least 83%) transcellular osmotic water pathway in the rabbit PCT.

External USL

In the proximal tubule external USL have been suggested by the presence of streaming potentials (Frömter et al., 1969; Corman, 1985). However, their values are small (<1 mV) and it is difficult to differentiate between the potential attributed to the presence of a USL and electrokinetic potentials induced by true solvent drag. A direct evaluation of the role of external USL in the measurement of P_f requires examination of P_f as a function of time, ambient solution mixing, or ambient solution diffusion coefficient (Barry & Diamond, 1984). However, in the present studies variation of bath and luminal solution flow rate and variation of bath viscosity failed to provide evidence for a bathing or luminal solution USL, probably because of adequate mixing and lack of surrounding supportive tissue.

Cytoplasmic USL

Failure to find evidence for an external USL suggests that a cytoplasmic or intracellular USL might be playing a role in the $\Delta\Pi$ dependence of apparent P_f. The presence of a cytoplasmic USL was originally suggested by Dick (1966) in sea urchin eggs because of the inverse dependence of P_f on cell size. More recently, a cytoplasmic USL has been suggested to account for $\Delta\Pi$ dependence of P_f by Barry and Diamond (1984) and Persson and Spring

(1982). Until recently there has been no experimental evidence supporting such a notion. Rick and DiBona (1987) have now measured an intracellular solute gradient during ADH-induced osmotic water flow using electron-microprobe analysis of freeze-dried cryosections in the toad urinary bladder. A major implication of this finding is that there is a significant cytoplasmic resistance to solute diffusion. Consequently, in the presence of transcellular water movement, the cell cytoplasm is not equiosmotic, but rather there is an osmotic profile across the cell cytoplasm. In contrast, other recent evidence in the ADH-treated mammalian cortical collecting duct contradicts this view (Strange & Spring, 1987).

Simple Cytoplasmic USL

In Appendix I the influence of a simple cytoplasmic USL on apparent P_f and on its $\Delta\Pi$ dependence were analyzed. Interestingly, although a simple cytoplasmic USL does result in an underestimate of P_f, it does not result in significant $\Delta\Pi$ dependence of P_f for the model parameters chosen to simulate the experimental protocol. This is understandable conceptually. A large osmotic gradient (e.g. 100 mOsm; perfusate 300 mOsm, bath 400 mOsm) will induce a large transepithelial volume flux causing solute polarization in the USL and a decreased osmotic driving force (e.g. osmolarities at the membrane surface of 330 and 370 mOsm). A small osmotic gradient (e.g. 1 mOsm; perfusate 300 mOsm, bath 301 mOsm) will induce a smaller transepithelial volume flux giving proportionately lower solute polarization (e.g. osmolarities at the membrane surface of 300.3 and 300.7 mOsm). But in both cases the fractional decrease in osmotic driving force is similar (40 out of 100 mOsm and 0.4 out of 1 mOsm). The marked dependence of apparent P_f on $\Delta\Pi$ is thus not explained by a simple USL. Conversely and importantly, these calculations indicate that a simple external or cytoplasmic USL *cannot be ruled out* from measurements of the $\Delta\Pi$ dependence of P_f. A simple USL gives a falsely low P_f, but does not give $\Delta\Pi$ dependence. For a USL to give $\Delta\Pi$ dependence the properties (average solute diffusion coefficient and/or the area available for volume flow) must change with $\Delta\Pi$. Such a USL will be referred to as a complex USL.

The increase in apparent E_a with increasing $\Delta\Pi$ provides experimental evidence against a simple cytoplasmic USL. For a transepithelial water transport pathway that includes cell membranes and USL in series, the apparent E_a is a combination of E_a for the membrane component and E_a for the USL. The E_a of a simple USL is approximately equal to the E_a for solute diffusion in unrestricted solution, 4–5 kcal/mole. Thus as $\Delta\Pi$ increases, the apparent E_a should tend toward 4–5 kcal/mole. Table 3 shows that the apparent E_a for osmosis in the rabbit PCT is 7.0 kcal/mole when $\Delta\Pi$ was 20 mOsm and 12.5 kcal/mole when $\Delta\Pi$ was 60 mOsm. This observation is not consistent with an increasing contribution of a simple USL when $\Delta\Pi$ increases. A simple USL, either external or cytoplasmic, therefore, does not appear to account for the $\Delta\Pi$ dependence of apparent P_f.

Complex Cytoplasmic USL

Using the present model parameters and the data at $\Delta\Pi$ of 20 mOsm, the experimental data at 60 and 100 mOsm cannot be modeled if the average solute diffusion coefficient D and the area available for flow are independent of $\Delta\Pi$ or the rate of transepithelial volume flow. The data can be modeled if D or the area available for flow decreased with increasing transepithelial volume flow. Using the parameters in the legend to Fig. 2, the decreased apparent P_f at an 80 mOsm gradient could be explained if the factor d/SD increased eight-fold (or equivalently, if the diffusion coefficient or the area available for flow decreased eight-fold). Such dependences are quite plausible physically. Transcellular volume flow may cause polarization of cytoplasmic contents (proteins, small organelles) with build-up at the surface to which flow is directed. The increased density of cytoplasmic material could decrease the area available for osmosis by presenting a physical barrier, or cause a decrease in solute diffusion coefficient. Using the Carmen-Kozeny equation for P_f in a 3-dimensional fiber matrix as described by Curry and Michel (1980), P_f is proportional to $f^3/(1-f)^2$ where f is the fraction of the total volume which is fluid and conductive to osmosis. This steep dependence of P_f on f suggests that a modest drop in f (e.g. 0.8 to 0.4) with cytoplasmic polarization could decrease 'cytoplasmic P_f' dramatically (72-fold), presenting a significant flow-dependent barrier to osmosis.

Although the data presented here do not provide direct evidence for a complex USL, the proposed physical mechanisms can be subjected to experimental verification. Measurement of pre-steady-state values for transepithelial P_f may provide evidence for solute polarization within the cell cytoplasm (Barry & Diamond, 1984). In addition, effects of transcellular flow on cytoplasmic polarization and on solute diffusion coefficient may be resolvable by quantitative fluorescence microscopy.

Role of Other Factors in ΔΠ Dependence of Apparent P_f

Change in Membrane Surface Area

A change in available membrane surface with changes in transepithelial volume flux predicts a ΔΠ dependence for P_f. An increase in the available membrane surface area due to unfolding of microvilli might be expected to increase apparent P_f. To explain the data surface area would have to increase with decreasing ΔΠ. However, if membrane surface area increases as ΔΠ goes from 60 to 20 mOsm, it is predicted that ΔΠ should have no effects on E_a and the inhibitory potency *p*CMBS, contrary to the experimental results. A change in membrane surface areas, thus, appears an unlikely explanation for the ΔΠ dependence of apparent P_f in the rabbit PCT.

Role of Saturable Water Transport Mechanism

A nonlinear relationship between flux and driving force is compatible with a carrier-mediated transport process. Carrier-mediated transport processes show saturation and can be described by a saturable, single-site model. For symmetrical, saturable water transport, the dependence of apparent P_f (P_f^{app}) on the absolute value of the osmotic gradient might be described by the relation, $P_f^{app} = P_f^{sat}\ \Delta\Pi/(\Delta\Pi + K_d) + P_f^{nonsat}$, where P_f^{sat} and P_f^{nonsat} are the magnitudes of saturable and nonsaturable water permeability, and K_d is an effective 'affinity' (Illsley & Verkman, 1986). The data in Table 1 are fitted well to this relation with a K_d of 10 mOsm.

Experimentally, the ΔΠ dependence of E_a (Table 3) is consistent with a saturable water transport pathway with a low E_a in parallel with a nonsaturable water transport pathway through membrane lipid with high E_a. However, other experimental data do not support the saturable water transport model. It would be expected that the inhibitory potency of *p*CMBS should change little once saturation of the water transporter has been achieved (>10 mOsm). However Table 2 shows that *p*CMBS inhibited apparent P_f strongly (83%) at a ΔΠ of 20 mOsm and insignificantly at a ΔΠ of 60 mOsm. In addition, saturation of a water transport pathway has not been observed in studies of the ΔΠ dependence of P_f in isolated brush border membrane vesicles (Verkman, Dix & Selfter, 1985; Chen et al., 1988) and in suspended rabbit proximal tubule cells (Meyer & Verkman, 1987). Furthermore, although transport saturation is easy to visualize for carrier-mediated solute transport, it is less so when considering osmotic water transport. One possible physical description of a saturable water transport mechanism might be a diminution of water flow as turbulent flow is approached. However, estimates of the Reynold's number for the water channel[3] do not support this possibility. Moreover, there is reasonably good agreement between the estimated single-channel P_f and that expected from Poiseuille's Law (Finkelstein, 1987), which suggests that even in channels as narrow as gramicidin A, where single-file diffusion of 5 water molecules is the currently accepted mode of water transport, laminar flow, rather than turbulent flow, prevails. Therefore it is unlikely that the ΔΠ dependence of apparent P_f is due to saturation of a symmetrical water transport pathway with a K_d of 10 mOsm.

Role of Physiologic Down-Regulation of Water Transport

ΔΠ dependence of apparent P_f could be explained by ΔΠ-dependent, physiologic down-regulation of water transport. Up- and down-regulation of P_f has been extensively studied in antidiuretic hormone (ADH)-sensitive epithelia, and involves, in part, the endocytic retrieval of water-permeable patches from the apical surface (Harris, Wade & Handler, 1986; Verkman et al., 1988). This type of process may have relevance to the proximal tubule. In the toad bladder ADH-stimulated osmotic water flow is initially proportional to the applied osmotic gradient, but P_f decreases with continued ADH and osmotic gradient exposure. The time-dependent decrease in P_f has been termed flux inhibition.

The present studies cannot address physiologic down-regulation of apparent P_f because between each experimental period there was a 15-min equilibration time. Direct evidence that the ΔΠ dependence of apparent P_f in the proximal tubule is due to

---

[3] To calculate the Reynolds number (R) for a single Gramicidin A channel represented by a right cylinder whose radius is 2Å, one needs to know v, the average velocity in the channel (cm/sec), D, the diameter of the channel (cm), p, the density of water (g/cm²), and n, the viscosity of water (dynes sec/cm²): $R = vDp/n$. v can be estimated from the single-channel P_f (6×10^{-14} cm³/sec per channel; Table 8-1, Finkelstein, 1987), the partial molar volume of water V_w (0.018 liter/mole) and the concentration gradient, C (100 mOsm):

$$v = [P_f V_w C]/[\pi r^2].$$

v is calculated to be 0.05 cm/sec. Using the diameter of the Gramicidin A channel (D) of 4×10^{-8} cm, the density of water at 25°C (p) 0.997 g/cm³, and the viscosity of water (n) 0.0089 dynes sec/cm², R is calculated to be 10^{-7}. Turbulent flow occurs when R is greater than 1000.

down-regulation of P_f requires rapid measurements of P_f immediately following osmotic gradient exposure. The present E_a and *p*CMBS data, however, are consistent with down-regulation if the down-regulated pathway is *p*CMBS sensitive and has an E_a of 7 kcal/mole.

In summary, we have determined the apparent P_f of the rabbit PCT at 20, 60 and 100 mOsm gradients and found a marked $\Delta\Pi$ dependence of apparent P_f sufficient to account for the wide range of transepithelial P_f reported previously. Mechanistically, the $\Delta\Pi$ dependence, or so-called nonlinear osmosis, could be explained by USL, change in surface area, saturation of water transport and down-regulation. A simple external or cytoplasmic unstirred layer, a flow-dependent change in surface area and saturation of a water transport pathway are unlikely on experimental and theoretical grounds. The present data are consistent with a complex cytoplasmic USL with flow-dependent characteristics. The role of down-regulation of apparent P_f is an interesting hypothesis that requires further investigation.

This work was supported by grants DK26142, DK35124 and DK39354 from the National Institutes of Health. ASV is an established investigator of the American Heart Association.

References

Altamirano, M., Martinoya, C. 1966. The permeability of the gastric mucosa of dog. *J. Physiol. (London)* **184:**771–790

Al-Zahid, G., Schafer, J.A., Troutman, S.L., Andreoli, T.E. 1977. Effect of antidiuretic hormone on water and solute permeation, and the activation energies for these processes, in mammalian cortical collecting tubules. Evidence for parallel ADH-sensitive pathways for water and solute diffusion in luminal plasma membranes. *J. Membrane Biol.* **31:**103–129

Andreoli, T.E., Schafer, J.A., Troutman, S.L. 1978. Perfusion rate-dependence of transepithelial osmosis in isolated proximal convoluted tubules: Estimation of hydraulic conductance. *Kidney Int.* **14:**263–269

Barry, P.H., Diamond, J.M. 1984. Effects of unstirred layers on membrane phenomena. *Physiol. Rev.* **64:**763–872

Bentley, P.J. 1961. Directional differences in the permeability to water of the isolated urinary bladder of the toad, *Bufo marinus*. *J. Endocrinol.* **22:**95–100

Bentzel, C.J., Parsa, B., Hare, D.K. 1969. Osmotic flow across proximal tubule of *Necturus;* correlation of physiologic and anatomic studies. *Am J. Physiol.* **217:**570–580

Berry, C.A. 1983. Water permeability and pathways in the proximal tubule. *Am. J. Physiol.* **245:**F279–F294

Berry, C.A. 1985. Characteristics of water diffusion in the rabbit proximal convoluted tubule. *Am. J. Physiol.* **249:**F729–F738

Brodsky, W.A., Schilb, T.P. 1965. Osmotic properties of isolated turtle bladder. *Am. J. Physiol.* **208:**46–57

Capri-Medina, P., Gonzalez, E., Whittembury, G. 1983. Cell osmotic water permeability of isolated rabbit proximal convoluted tubules. *Am. J. Physiol.* **244:**F554–F563

Chen, P.Y., Pearce, D., Verkman, A.S. 1988. Membrane water and solute permeability determined quantitatively by self-quenching of an entrapped fluorophore. *Biochemistry* **27:** 5713–5718

Corman, B. 1985. Streaming potentials and diffusion potentials across rabbit proximal convoluted tubule. *Pfluegers Arch.* **403:**156–163

Corman, B., DiStefano, A. 1983. Does water drag solutes through kidney proximal tubule? *Pfluegers Arch.* **397:**35–41

Curry, F.E., Michel, A.E. 1980. A fiber matrix model of capillary permeability. *Microvasc. Res.* **20:**96–99

Dainty, J. 1963. Water relations of plant cells. *Adv. Bot. Res.* **1:**279–326

Dainty, J., Ginzburg, 1964. The measurement of hydraulic conductivity (osmotic permeability to water) of internodal characean cells by means of transcellular osmosis. *Biochim. Biophys. Acta* **79:**102–111

Diamond, J.M. 1966. Non-linear osmosis. *J. Physiol. (London)* **183:**83–100

Diamond, J.M. 1979. Osmotic water flow in leaky epithelia. *J. Membrane Biol.* **51:**195–216

Dick, D.A.T. 1959. Osmotic properties of living cells. *Int. Cyto.* **8:**387–448

Dick, D.A.T. 1966. Cell Water. Butterworths, Seattle, Washington

DuBois, R., Verniory, A., Abramow, M. 1976. Computation of the osmotic water permeability of perfused tubule segments. *Kidney Int.* **10:**478–479

Earley, L.E., Sidel, V.W., Orloff, J. 1962. Factors influencing permeability of vasopressin-sensitive membrane. *Fed. Proc.* **21:**145

Finkelstein, A. 1987. Water Movement Through Lipid Bilayers, Pores, and Plasma Membranes. Theory and Reality. John Wiley and Sons, New York

Franz, T.J., Van Bruggen, J.T. 1967. Hyperosmolarity and the net transport of nonelectrolytes in frog skin. *J. Gen. Physiol.* **50:**933–949

Frömter, E., Muller, C.W., Knauf, H. 1969. Fixe negative wandladungen im proximalen konvolut der rattenniere und thre beeinflussung durch calcuimionen. *In:* Aktuelle Probleme des Elektroyte- und Wasserhaushaltes, Nierenbiopsie. B. Watschinger, editor. pp. 61–64. Wiener Medizinischen Akademie, Vienna

Harris, H.W., Wade, J.B., Handler, J.S. 1986. Transepithelial water flow regulates apical membrane retrieval in antidiuretic hormone-stimulated toad urinary bladder. *J. Clin. Invest.* **78:**703–712

Harris, S.I., Patton, L., Varrett, L., Mandel, L.J. 1982. (Na^+,K^+)-ATPase kinetics within the intact renal cell. The role of oxidative metabolism. *J. Biol. Chem.* **257:**6996–7002

Heeswijk, M.P.E. van, Os, C.H. van, 1986. Osmotic water permeabilities of brush border and basolateral membrane vesicles from rat renal cortex and small intestine. *J. Membrane Biol.* **92:**183–193

House, C.R. 1974. Water Transport in Cells and Tissues. Williams and Wilkins, Baltimore, Maryland

Illsley, N.P., Verkman, A.S. 1986. Serial permeability barriers to water transport in human placental vesicles. *J. Membrane Biol.* **94:**267–278

Kedem, O., Katchalsky, A. 1963. Permeability of composite membranes. Part 3. Series array of elements. *Trans. Faraday Soc.* **59:**1941–1953

Kokko, J.P., Burg, M.B., Orloff, J. 1971. Characteristics of NaCl and water transport in the renal proximal tubule. *J. Clin. Invest.* **50:**69–76

Loeschke, K., Bentzel, C.J., Caaky, T.Z. 1970. Assymmetry of osmotic flow in frog intestine; functional and structural correlation. *Am. J. Physiol.* **218:**1723–1731

Macey, R.I., Daran, D.M., Farmer, R.E.L. 1972. Properties of water channels in human red cells. *In:* Passive Permeability of Cell Membranes. Biomembranes 3. F. Kreuzer and J.F.G. Slegers, editors. pp. 331–340. Plenum, New York

Meyer, M.M., Verkman, A.S. 1987. Evidence for water channels in renal proximal tubule cell membranes. *J. Membrane Biol.* **96:**107–119

Ogilvie, J.T., McIntosh, J.R., Curran, P.F. 1963. Volume flow in a series-membrane system. *Biochim. Biophys. Acta* **66:**441–444

Patlak, C.S., Goldstein, D.A., Hoffman, J.F. 1963. The flow of solute and solvent across a two-membrane system. *J. Theor. Biol.* **5:**426–442

Persson, B., Spring, K.R. 1982. Gallbladder epithelial cell hydraulic water permeability and volume regulation. *J. Gen. Physiol.* **79:**481–505

Pratz, J., Ripoche, P., Corman, B. 1986. Evidence for proteic water pathways in the luminal membrane of kidney proximal tubule. *Biochim. Biophys. Acta* **856:**259–266

Ramsay, J.A., Brown, R.H.J. 1955. Simplified apparatus and procedure for freezing-point determinations upon small volumes of fluid. *J. Sci. Instrum.* **32:**372–375

Rick, R., DiBona, D.R. 1987. Intracellular solute gradients during osmotic water flow: An electron-microprobe analysis. *J. Membrane Biol.* **96:**85–94

Schafer, J.A., Patlak, C.S., Andreoli, T.E. 1978. Volume absorption in the pars recta. II. Hydraulic conductivity coefficient. *Am. J. Physiol.* **234:**F340–F348

Skadhauge, E. 1967. In vivo perfusion studies of the cloacal water and electrolyte resorption in the fowl (*Gallus domesticul*). *Comp. Biochem. Physiol.* **23:**483–501

Strange, K., Spring, K.R. 1987. Absence of significant cellular dilution during ADH-stimulated water reabsorption. *Science* **235:**1068–1070

Ullrich, K.J. 1972. Permeability characteristics of the mammalian nephron. *In:* Handbook of Physiology. Renal Physiology. J. Orloff and R.W. Berliner, editors. pp. 377–398. American Physiol. Society, Washington, DC

Verkman, A.S., Dix, J.A., Selfter, J.L. 1985. Water and urea transport in renal microvillus membrane vesicles. *Am. J. Physiol.* **248:**F650–F655

Verkman, A.S., Lencer, W.I., Brown, D., Ausiello, D.A. 1988. Endosomes from kidney collecting tubule contain the vasopressin-sensitive water channel. *Nature* **333:**268–269

Verkman, A.S., Wong, K.R. 1987. Proton nuclear magnetic resonance measurement of diffusional water permeability in suspended renal proximal tubules. *Biophys. J.* **51:**717–723

Wang, J.H. 1954. Theory of self-diffusion of water in protein solutions. A new method for studying the hydration and shape of protein molecules. *J. Am. Chem. Soc.* **19:**4755–4763

Whittembury, G., Capri-Medina, P., Gonzalez, E., Linares, H. 1984. Effect of para-chloromercuribenzenesulfonic acid and temperature on cell water osmotic permeability of proximal straight tubules. *Biochim. Biophys. Acta* **775:**365–373

Wright, E.M., Smulders, A.P., Tormey, J.M. 1972. The role of the lateral intercellular spaces and solute polarization effects in the passive flow of water across the rabbit gallbladder. *J. Membrane Biol.* **7:**198–219

Received 24 November 1987; revised 13 May 1988

Appendix

I. One-Dimensional Cytoplasmic Unstirred Layer

Consider a cell separating solutions 1 and 2 containing solute with bulk concentrations C_1 and C_2 (Fig. 4). Within the USL (cell cytoplasm), solute polarization will diminish the driving force for osmotic water flux (J_v) by altering solute concentration just within the cell (C_1^m and C_2^m) according to the relations (Barry & Diamond, 1984),

$$C_1^m = C_c\exp(-J_v d/SD) \qquad C_2^m = C_c\exp(J_v d/SD) \tag{A1}$$

where d is the USL thickness (cm) (*see* Fig. 4), D is solute diffusion coefficient in the USL (cm²/sec), S is tubule surface area (cm²/mm) and C_c is solute concentration midway within the cell (mM). Steady-state mass conservation requires that,

$$J_v = P_f^m V_w S(C_2 - C_2^m) = P_f^m V_w S(C_1^m - C_1) \tag{A2}$$

where P_f^m is the osmotic water permeability of the individual apical and basolateral membranes in cm/sec (assumed to be equal), and V_w is the partial molar volume of water.

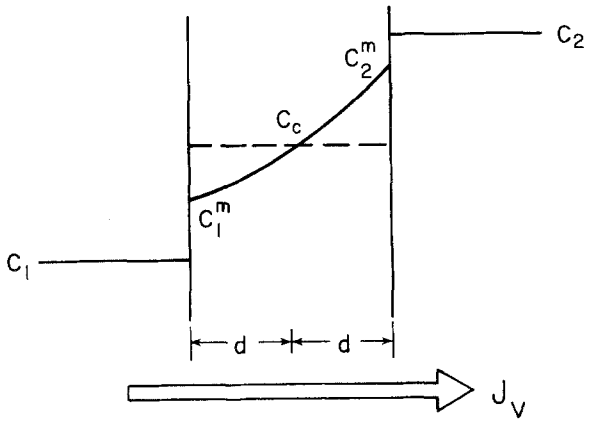

Fig. 4. Schematic of cell with cytoplasmic unstirred layer separating solutions 1 and 2. Bulk solute concentrations C_1 and C_2 are constant in the absence of an external USL. Within the cell cytoplasm, convection-diffusion causes solute polarization with solute concentrations C_1^m and C_2^m at the cell cytoplasm-membrane boundary. The dashed line shows the predicted solute concentration in the absence of solute polarization in which the osmotic water permeabilities of the two membranes are equal

Combining Eqs. (A1) and (A2),

$$J_v = P_f^m V_w S(C_2 - [C_1 + C_2]/[1 + \exp(-2J_v d/SD)]). \quad \text{(A3)}$$

Equation (A3) was solved iteratively for J_v using Newton's method. The apparent transepithelial water permeability (P_f) is then,

$$P_f = J_v/[V_w S(C_1 - C_2)]. \quad \text{(A4)}$$

II. Two-Dimensional Cytoplasmic Unstirred Layer

The two-dimensional analog of Eq. (A3) was derived to better approximate tubule geometry. In general, the steady-state convection-diffusion equation is,

$$D \nabla^2 C = \mathbf{v} \cdot \nabla C \quad \text{(A5)}$$

where $\mathbf{v}$ is flow velocity. In two dimensions with cylindrical symmetry in which flow is radial and in which all intracellular volume accommodates volume flow,

$$D \frac{d^2C}{dr^2} + \frac{1}{r}\frac{dC}{dr} = J_v(r) \frac{dC}{dr}. \quad \text{(A6)}$$

If the inner and outer tubule radii are r_1 and r_2, respectively, $J_v(r)$ will be taken to be $J_v(r_o) \cdot (r_o/r)$, where r_o is midway in the cell, to account for the radial convergence of flow and allow for analytical integration. Integration of Eq. (A6) for an impermeant solute subject to the condition $C(r_o) = C_c$ gives the relations analogous to Eq. (A1),

$$C_1^m = C_c(1 - d/r_o)^{(r_o - d)J_v(r_o)/SD} \quad \text{(A7)}$$

$$C_2^m = C_c(1 + d/r_o)^{(r_o + d)J_v(r_o)/SD}.$$

Applying mass conservation, the two-dimensional relationship analogous to Eq. (A3) is,

$$J_v(r_o) = P_f^m S V_w (r_2/r_o)\left[C_2 - \frac{C_2 + (r_1/r_2)C_1}{1 + \frac{r_1(1 - d/r_o)^{(r_o - d)J_v(r_o)/SD}}{r_2(1 + d/r_o)^{(r_o + d)J_v(r_o)/SD}}}\right] \quad \text{(A8)}$$

where $r_o = (r_1 + r_2)/2$. The relationship between P_f and $C_2 - C_1$ is then given approximately by Eq. (A4) with J_v replaced by $J_v(r_o)$.